

Article

Comparative Traffic Flow Prediction of a Heuristic ANN Model and a Hybrid ANN-PSO Model in the Traffic Flow Modelling of Vehicles at a Four-Way Signalized Road Intersection

Isaac Oyeyemi Olayode ^{1,*}, Lagouge Kwanda Tartibu ¹, Modestus O. Okwu ¹ and Alessandro Severino ²

¹ Department of Mechanical and Industrial Engineering, University of Johannesburg, Johannesburg P.O. Box 2028, South Africa; ltartibu@uj.ac.za (L.K.T.); okwu.okechukwu@fupre.edu.ng (M.O.O.)

² Department of Civil Engineering and Architecture, University of Catania, 95123 Catania, Italy; alessandro.severino@unict.it

* Correspondence: olayode89@gmail.com; Tel.: +27-710200947

Abstract: The accurate and effective prediction of the traffic flow of vehicles plays a significant role in the construction and planning of signalized road intersections. The application of artificially intelligent predictive models in the prediction of the performance of traffic flow has yielded positive results. However, much uncertainty still exists in the determination of which artificial intelligence methods effectively resolve traffic congestion issues, especially from the perspective of the traffic flow of vehicles at a four-way signalized road intersection. A hybrid algorithm, an artificial neural network trained by a particle swarm optimization model (ANN-PSO), and a heuristic Artificial Neural Network model (ANN) were compared in the prediction of the flow of traffic of vehicles using the South Africa transportation system as a case study. Two hundred and fifty-nine (259) traffic datasets were obtained from the South African road network using inductive loop detectors, video cameras, and GPS-controlled equipment. For the ANN and ANN-PSO training and testing, 219 traffic data were used for the training, and 40 were used for the testing of the ANN-PSO model, while training (160), testing (40), and validation (59) was used for the ANN. The ANN result presented a logistic sigmoid transfer function with a 13–6–1 model and a testing R^2 of 0.99169 compared to the ANN-PSO result, which showed a testing performance of R^2 0.99710. This result shows that the ANN-PSO model is more efficient and effective than the ANN model in the prediction of the traffic flow of vehicles at a four-way signalized road intersection. Furthermore, the ANN and ANN-PSO models are robust enough to predict traffic flow due to their better testing performance. The modelling approaches proposed in this study will assist transportation engineers and urban planners in designing a traffic control system for traffic lights at four-way signalized road intersections. Finally, the results of this research will assist transportation engineers and traffic controllers in providing traffic flow information and travel guidance for motorists and pedestrians in the optimization of their travel time decision-making.

Keywords: artificial neural network; particle swarm optimization; traffic congestion; artificial intelligence; artificial neural network-particle swarm optimization; traffic flow; signalized road intersection



Citation: Olayode, I.O.; Tartibu, L.K.; Okwu, M.O.; Severino, A. Comparative Traffic Flow Prediction of a Heuristic ANN Model and a Hybrid ANN-PSO Model in the Traffic Flow Modelling of Vehicles at a Four-Way Signalized Road Intersection. *Sustainability* **2021**, *13*, 10704. <https://doi.org/10.3390/su131910704>

Received: 12 August 2021

Accepted: 21 September 2021

Published: 27 September 2021

Publisher's Note: MDPI stays neutral with regard to jurisdictional claims in published maps and institutional affiliations.



Copyright: © 2021 by the authors. Licensee MDPI, Basel, Switzerland. This article is an open access article distributed under the terms and conditions of the Creative Commons Attribution (CC BY) license (<https://creativecommons.org/licenses/by/4.0/>).

1. Introduction

In developed and developing countries, traffic congestion at signalized road intersections has become a central issue. Efficient and effective traffic flow prediction in road transportation is one of the most fundamental characteristics of smart cities and intelligent transportation systems [1]. It is imperative to transportation researchers and pedestrians [1]. Having up-to-date traffic flow information for traffic congestions on freeways and knowing the level of the traffic volume of vehicles at road intersections in advance plays an important role in assisting transportation and civil engineers in developing and

implementing transportation planning strategies, improving the efficiency of traffic network operations, and reducing the problem of traffic congestions on freeways and road intersections. Another advantage of having up-to-date traffic flow information is that it assists road users in orientating the travel routes to use when traveling to avoid getting stuck in traffic. It also reduces travel times on the road.

Therefore, these advantages listed above have made traffic flow prediction an indispensable branch of road transportation and have attracted attention from various transportation researchers over the last few decades. However, transportation researchers have made many attempts to improve traffic flow prediction using outdated and classical models. Many have applied traditional statistical techniques to predict traffic flow problems in the last 20 years, such as the Autoregressive Integral Moving Average (ARIMA) [2]. This traditional model is only appropriate for traffic flow predictions that are linear in nature and stable [3]. Other traditional models—such as the Support Vector Machine (SVM) [4], Support Vector Regression Machine (SVR) [5,6], Bayesian method [7], and K-nearest neighbour [8]—are models which are all applied in traffic flow prediction, with the aim of processing non-linear traffic datasets. Still, their prediction performance depends on cautious characteristic engineering, making these models inapplicable to the Spatio-temporal correlation analysis of traffic flow datasets.

Over the last few years, many machine-learning methods have been used to address the problems of traffic flow predictions. A typical example of this is when [9] applied a Graph Convolutional Network (GCN) to accurately extract the spatial characteristics of a traffic road network. However, all of these traditional statistical methods have yielded positive results in the prediction of traffic flow. However, past related research has shown that most of these neural networks still lack accuracy and effectiveness in terms of regression values when compared to heuristics and hybrid models.

Research findings, over the years, have proven that traditional models cannot handle a large volume of traffic data. One major theoretical issue that has dominated the field of transportation for many years is that if a large volume of traffic datasets is not handled (divided into inputs and outputs) properly, this can decrease the accurate prediction of traffic flow at road intersections or freeways. ANN-PSO was used in this study because many researchers have used particle swarm optimization modelling to develop a predictive approach in different areas of studies; notably, among them is [10], who used the ANN-PSO model to predict thermal properties; [11] used different types of particle swarm optimization algorithms, such as basic particle swarm optimization (PSO), to find solutions to three primary aspects (synaptic weights, architecture, and transfer functions neurons) of an ANN network. [12] used another form of hybrid particle swarm optimization called social learning particle swarm optimization (SL-PSO) to solve real-time traffic signal control. During this research, it was discovered that a hybrid ANN-PSO model, to the best of the author's knowledge, has never been used before to predict or model the traffic flow performance of vehicles at four-way signalized road intersections.

1.1. Motivation and Contribution of the Research

The primary reason why a hybrid ANN-PSO was used in this study was that [12] stated that PSO can be defined as an optimization technique that performs a rapid convergence to optimal performances. This characteristic is desirable when evaluating different traffic conditions (traffic flow, traffic density, and vehicular speed). Besides this, a canonical PSO algorithm is easy to use and requires very few adjustment parameters. The main objective of this study was to carry out an extensive comprehensive analysis of the prediction performance of the traffic flow of vehicles by comparing the traffic flow prediction performance of a heuristic ANN model and a hybrid ANN-PSO model. Another primary objective of this research study was to examine the emerging role of soft computing techniques (ANN and ANN-PSO) in the context of traffic flow modelling at a signalized road intersection. This research study will provide a significant opportunity to advance the understanding of the application of an artificial neural network model (ANN) and

an artificial neural network trained by particle swarm optimization (ANN-PSO) in the modelling of the traffic flow of vehicles at a four-way signalized road intersection. Another significant contribution of this research is that it will assist various developed and developing countries to advance their traffic management techniques in curbing traffic congestion at road intersections.

1.2. Organization of the Research

This paper has been divided into five parts. The first part deals with the overview and significance of the study. The second part begins by laying out the theoretical dimensions of the research and looks at related studies on ANN and ANN-PSO. The third part is concerned with the methodology used in this research study and a detailed explanation of the traffic control delay at a four-way signalized road intersection. The fourth part presents the findings of the research. The final part draws upon the entire paper, tying up the various theoretical and empirical findings to contribute to the field of transportation, and areas for further research are identified.

2. Literature Review

2.1. Related Studies

In the last few years, transportation researchers have carried out a lot of research on the occurrence of traffic congestion in road transportation and the prediction of the traffic flow at various road networks. However, few researchers have drawn on any structured research into traffic flow prediction at signalized road intersections using hybrid and heuristic predictive models. Previous studies by D'Andrea and his co-worker Marcelloni created an expert system for detecting traffic congestions at various road networks by using traffic data that comprises the past and current vehicular speed [13]. Related research to [13] was proposed by [14], in which a method called “scalable” was used to predict the traffic congestion of vehicles in a grid framework. Anwar and co-workers applied a spectral clustering-based method to supervise traffic congestions [15]. Considering the traffic flow density and different types of roads, Liang and co-workers developed a novel prediction model capable of estimating the next-time step traffic volume using a single road traffic segment to clarify traffic congestions using traffic flow variables such as the current inflow, outflow, and traffic volume, etc. [16].

However, the research carried out by Xiangjie and co-workers improved the model of [16] by using a support vector machine (SVM) for the prediction of the next time-step traffic speed and traffic volume and used it in the estimation of traffic congestion of segments roads [17]. Researchers such as [18] proposed a specialized density-based spatial clustering application (DBSCAN) using a noise algorithm. This was developed for the detection and analysis of a consistent congested cluster of grids. They investigated a deep-learning-based prediction model using a restricted Boltzmann Machine and a Recurrent Neural Network to predict the traffic flow at congested roads [18]. A practical traffic flow parameter prediction model was created for traffic flow conditions estimations. An autoregressive model was combined with other predictive models [17,19]. In their research, [20] developed a model combining artificial neural networks and root mean squared error. Both were used as a metric by applying singular point probabilities. Traffic congestion has become a global pandemic that transportation researchers are racing against time to improve the effectiveness of intelligent transportation systems. Some researchers have been able to achieve good results when it comes to traffic flow prediction. Traffic flow prediction techniques are categorized into:

- Traditional statistical techniques.
- Traditional machine learning techniques.
- Deep learning methods.

Traditional statistical techniques comprise the historical average method (HA) and a statistical technique called Autoregressive Integrated Moving Average (ARIMA) [2]. Subsequently, the features of the ARIMA model consist of the combination of several models,

such as ARIMA time series models (KARIMA) [21] and the Seasonal Autoregressive Integrated Moving Average (SARIMA) [22]. However, the major disadvantage of this type of model is the limitation in the processing capacities in terms of non-linear and challenging traffic flow data [23].

Compared with the above traditional models, traditional machine learning techniques can efficiently model complex non-linear traffic data. Typical examples are SVM [4,24,25] and SVR [5,26]. These traditional models can map low-dimensional non-linear data to high-dimensional space using kernel functions to evaluate traffic data characteristics for prediction. However, the selection of the kernel function is a primary determinant affecting the performance of predictive models. Apart from Bayesian models [7], K nearest neighbours [8,27,28] and Artificial Neural Networks (ANN) [29] have been applied for the prediction of traffic flow. The significant drawback of traditional machine learning is their reliance on engineering and the experience of experts [30]. However, for these traditional methods, it is complex to improve the efficiency of these predictive models when processing and evaluating complex and highly non-linear data [3,31]. Currently, deep learning techniques in transportation have yielded good results, especially in image processing and natural language processing [32].

Nowadays, transportation researchers are applying deep learning methods in traffic data mining using temporal and spatial correlation. Previous research performed by [6,33], in which they applied Deep Belief Networks (DBN) and Stacked Autoencoder Models (SAEs) to extend and deepen the network layers for the learning of the features in traffic flow data. Then, researchers such as [34] applied the combination of traffic flow and weather information to enhance the predictive performance of the DBN model. Models such as Long Short-Term Memory (LSTM) [35–38], Gated Recurrent Unit Network (GRU) [39], and Nonlinear Autoregressive with External Input (NARX) [36] were applied for the temporal correlation of traffic flow data to improve the traffic flow prediction. However, these predictive models failed to consider the spatial relationship in the structure of the traffic network. Even though Convolutional Neural Networks (CNNs) [40–42] have made significant headway in the field of vision, transportation researchers went further in applying CNN to traffic flow prediction to capture local spatial characteristics. Hence, [43] suggested Deep Spatio-Temporal Residual Networks (STResNet) to predict the flow of people in a transportation system.

Few recent surveys have comprehensive literature reviews on traffic flow prediction in specific contexts from various perspectives of road transportation, especially from the traffic flow of vehicles at road intersections. For example, [44] investigated the techniques and applications from the past decade and explained in detail the ten challenges and issues experienced by pedestrians and motorists in terms of traffic flow. The investigations carried out by [44] were more aimed at considering short-term traffic flow prediction. The literature reviews involved were primarily dependent on the conventional methods of traffic flow prediction. Another piece of research by [45] focused on the prediction of short-term traffic flow by summarizing the methods applied in the prediction of traffic flow. They also made some cogent suggestions for future research.

Furthermore, research carried out by [46] explained, in detail, how to acquire traffic data and aimed their research at conventional machine learning techniques. In addition to these, [47] indicated the contributions and research frameworks of traffic flow prediction. The research carried out by [48–51] summarized the applicable models that depend on conventional techniques and some early deep learning techniques. Alexander et al. [52] outlined a comprehensive survey of deep neural networks to predict the traffic flow of vehicles. Their research discussed three well-known deep neural architectures comprising convolutional, recurrent, and feed-forward neural networks. However, some recent technological innovations involving graph-based deep learning were not discussed in their research [52]. Likewise, researchers such as [53] investigated a well-detailed survey of graph-based deep learning architecture, including their applications in the field of traffic flow. Furthermore, [54], in their research, outline a survey aimed at applying deep learning

models in the evaluation and analysis of traffic flow data. However, their research neglects to focus on other areas of road transportation. They only carried out their investigations on the prediction of traffic flow. In general, there is other research on the prediction of traffic flow in road transportation that possesses standard features. It is always advantageous to consider all of the areas of traffic flow. Therefore, there is still insufficient research that contributes to traffic flow prediction, especially when it comes to traffic flow prediction using heuristics and nature-inspired algorithms.

Comparing different model specifications shows that testing results are significant in supporting the usefulness of a proposed prediction model. For example, [3] investigated the usefulness and effectiveness of recent comparative research based on short-term traffic flow forecasting. They stated that not all model comparisons are efficient, especially when comparing a complex non-linear model and a simple linear model. In addition, there exists an almost non-existent difference between the accuracy, simplicity, and suitability of a model (Occam's razor). In their research, [55] recommend that as much as model accuracy is very significant, it shouldn't only be used as a yardstick in determining the appropriate methodology for the prediction of the traffic flow of vehicles. Other challenges, such as time and effort, should be considered when determining the development of the model, techniques, and expertise, resulting from the transferability and suitability to changes in the temporal behaviour of traffic flow [55–57].

Even though choosing the "best" model in a group of baseline models using testing and comparison is significant, there is a need for a practical option to select a heuristic or metaheuristic approach to combine traffic flow predictions. The combination of predictive models may not likely result in a single well-specified model. A well-known case is the forecasting of complex traffic datasets. Different researchers in traffic flow forecasting have carried out this approach of combining predictive models; [58] carried out research in which they offered statistical guidelines for traffic flow by dynamically shifting between different models. The only disadvantage of their research is that they did not provide combined forecasts of traffic flow. Furthermore, [59] researched the combination of traffic flow forecasts from two neural networks by applying the Bayesian rule. In their research, [60] investigated the combination of traffic flow predictions from various types of predictive models, while [61] applied a fuzzy logic model to combine traffic flow forecasts. The research of [62] was based on combining forecasts from three models by applying neural networks.

2.2. Traffic Flow Patterns at a Signalized Road Intersection

This subsection describes the use of a time-space diagram (Figure 1) to explain the traffic flow patterns at a four-way signalized road intersection.

When drivers arrive at a signalized road intersection, the driver's response to traffic lights is important in understanding the traffic flow patterns at a road intersection, i.e., the response of drivers when the traffic lights turn red, the beginning of the traffic signal interval when the traffic lights turn green, and the queue of the vehicles clearing from the road intersection without any traffic control delays. This process continues back and forth from traffic lights turning to red, then to green, and back to yellow, then to red again. These are the basic concepts behind the traffic flow of vehicles at signalized road intersections. To explain these concepts efficiently, we are going to use a time-space diagram. Some assumptions were made trying to explain these time-space diagrams. These assumption diagrams can be found in the book written by [63].

Assumption 1

Let us assume that three vehicles are traveling at a uniform speed and are approaching a signalized road intersection. The "space" between the vehicles and the road intersection is shown on the y-axis, while the time is on the x-axis. The three circles display the traffic lights. These traffic lights can be either green, yellow, or red, depending on real-time traffic flow.

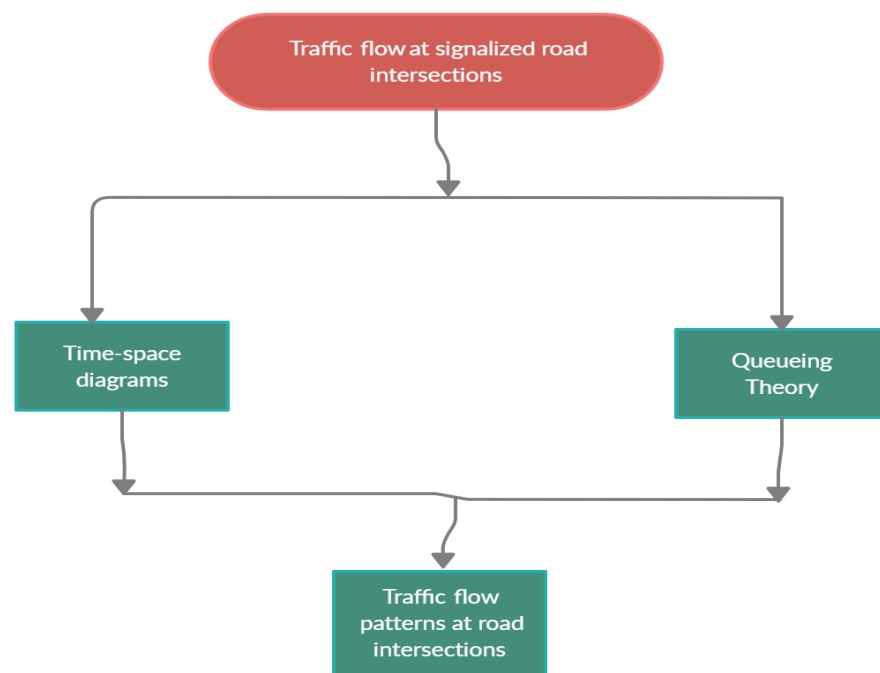


Figure 1. Fundamental concepts of traffic flow at a signalized road intersection.

Assumption 2

These three vehicles have been traveling at a uniform speed. These vehicles' trajectories are parallel and linear. The traffic lights turn red as these vehicles reach the road intersection.

Assumption 3

As the traffic lights turned red, the three vehicles approaching the intersections had to stop, and their speed dropped drastically. Two incoming vehicles meet the three vehicles at the road intersection, making it five vehicles in a queue at the intersection. Deceleration has occurred, and the vehicular speed is zero. In Assumption 3, as the speed of the vehicle drops due to the traffic lights turning red, the duration of time spent at the road intersection increases.

Assumption 4

As the traffic lights turn green, the vehicles already waiting in a queue at the road intersection start accelerating and driving into the intersection.

Assumption 5

The vehicles arriving at the road intersections after the queue has cleared will be delayed, as the traffic lights are still green.

Assumption 6

This is when vehicles arrive at the road intersections when the traffic lights turn yellow. Their speed gradually reduces as they drive towards the road intersection, as the traffic lights can turn red anytime.

Assumption 7

Now that the traffic lights have turned red, the incoming vehicles must stop and adhere to this traffic control delay and form a new queue.

Assumption 8

1. This is called the "traffic shockwaves" of the queues of vehicles forming at a road intersection when the traffic lights turn red.

2. This is a traffic shockwave of vehicles when the traffic lights turn green.
3. This is a traffic control delay for each vehicle at the intersection. This is the arrival time when vehicles arrive at a road intersection and when they leave the intersection.
4. This is when two vehicles depart at the same time from the road intersection. It is called “saturation headway”.
5. This is the speed of the vehicles as they arrived at and departed from the road intersection.
6. This is called the time gap. It usually occurs between the departing vehicle and the arriving vehicle.

Assumption 9

The driver responses at signalized road intersections are shown in the Assumption 9 diagrams using figures.

1. The driver stopped because the traffic light was red.
2. This is the driver driving through the intersection when the traffic light is green.
3. This is the driver driving through the intersection when the queue is cleared and no vehicles are waiting at the road intersection.
4. This is the driver reducing their speed because the traffic light has turned green.

3. Methodology

The workflow of the methodologies used in this research is shown in Figure 2.

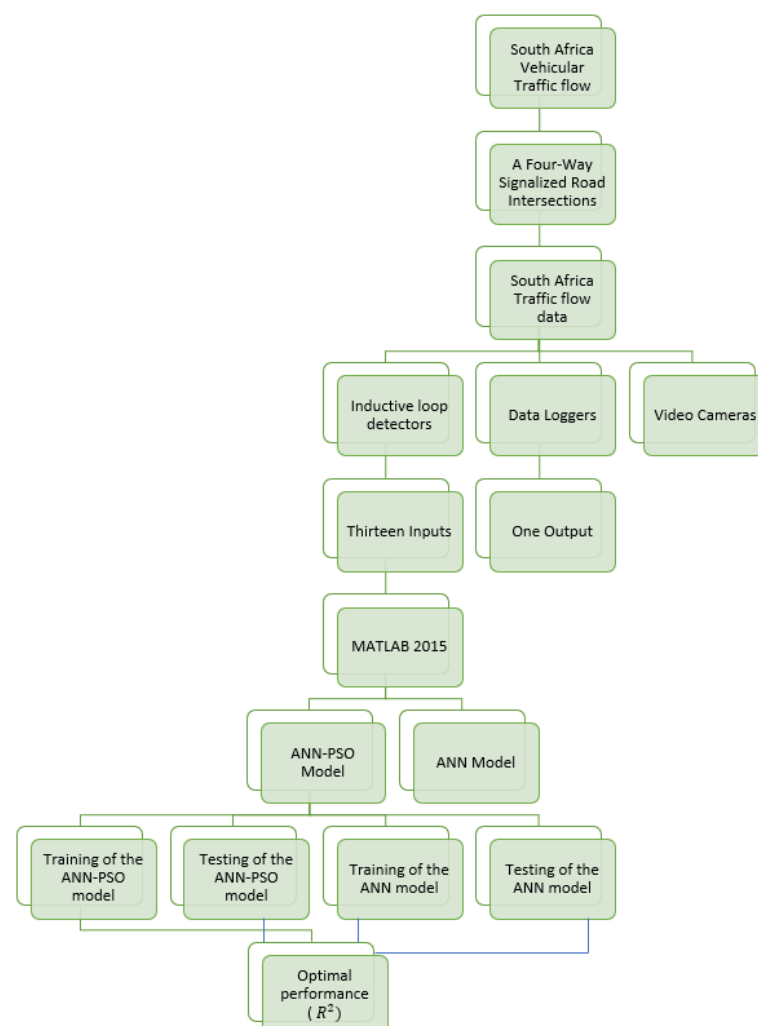


Figure 2. Research workflow.

3.1. Research Design

This research was designed to determine the ways in which issues of traffic congestion can be addressed from the perspective of the traffic flow at four-way signalized road intersections. This was achieved by designing a classical and generic traffic flow model for signalized road intersections, considering the selected metropolitan section of Gauteng province in South Africa. This research focused mainly on the qualitative and the quantitative techniques of addressing traffic congestion issues.

3.2. Population of the Research

One of the very few companies known for traffic monitoring solutions and traffic safety is the study's population. The company is known as Mikros Traffic Monitoring (MTM) Company, a subsidiary of the Syntell group of companies. This company works in conjunction with the South Africa Ministry of Transportation and South Africa National Roads Agency Limited (SANRAL).

3.3. Size of Traffic Data

The size of the dataset considered in this study is limited to 259 traffic datasets obtained from MTM, focusing on a four-way signalized road intersection within the investigation period.

3.4. Method of Traffic Data Collection

The technique used for the traffic data collection comprises primary and secondary techniques. The primary technique used in this study comprises the collection of traffic flow data from South African four-way signalized road intersections using inductive loop detectors, video cameras, and road-wide stationed GPS-controlled equipment. The secondary data has to do with direct visits to the Mikros Traffic Monitoring (MTM) Company and interaction with the strategic and operational staff of MTM to obtain information on traffic flow situations at various intersections.

3.5. Sample and Sampling Methods

Sampling is defined as the selection of a subcategory of samples from a statistical population to evaluate the traffic dataset. A fraction of two hundred and fifty-nine (259) datasets were selected to evaluate the traffic data's entirety, representing the vehicles manoeuvring at a four-way signalized road intersection in the Gauteng province within the investigation period. The traffic engineers in the South Africa Ministry of Transportation carried out the data cleaning on the traffic datasets to remove any duplication or unwanted traffic data.

3.6. Location of the Study

The input and output variables used for the ANN and ANN-PSO network are shown in Table 1. This input and output variable approach was based on the approach used by [64,65]. The preparation of the traffic dataset is followed by the structuring of the architecture of the algorithms. MATLAB user interface tools and command-line functionality were used to oversee the ANN and ANN-PSO models' development, training, and testing. The 259 traffic datasets used in this traffic prediction study were obtained from the N1: Allandale Interchange (Figure 3). This N1 interchange during the traffic flow peak period accommodates more than 90,000 automatic and manually driven vehicles traveling southbound and northbound and over 72,000 vehicles moving northbound every day. The N1 Allandale Interchange is a South African Government (National) road network that links Johannesburg through Pretoria, Bloemfontein, Polokwane, Capetown, and Beit Bridge. The traffic flow variables used for the development of the ANN and ANN-PSO model are listed in Table 1 and Figure 4 below:

Table 1. Categorization of the traffic datasets into the inputs and output.

Input Variables	Output Variables
Traffic density	Traffic Volume
The Number of light vehicles	
The average speed of light vehicles	
Time of day of light vehicles	
The average speed of a long truck	
Time of day of long truck	
Number of long trucks	
The average speed of a medium truck	
Time of day of medium truck	
The Number of medium trucks	
The Number of short trucks	
The average speed of a short truck	
Time of day of short truck	

**Figure 3.** The road intersection (Allandale Interchange).

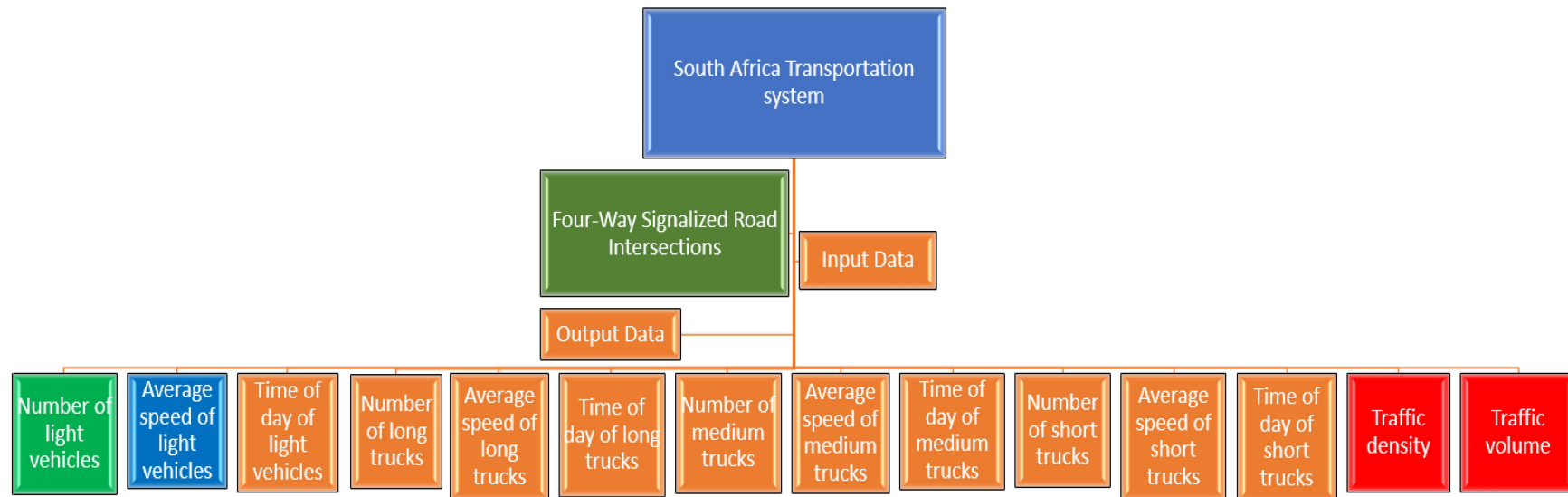


Figure 4. The South Africa transportation system traffic datasets.

3.7. Collection and Extraction of the Traffic Datasets

This research study collected traffic datasets from a four-way signalized road intersection which is located on Johannesburg to Pretoria Road, one of Southern Africa's busiest roads. Each roadsite has a different number of lanes, and they all move in the southbound direction. For the present study, only one direction of traffic was considered: the southbound direction. The inductive loop detector and video cameras were permanently installed at each of the four road intersections to obtain the necessary traffic data for the ANN and ANN-PSO model training, testing, and validation. Traffic flow data was collected from video cameras and inductive loop detectors for fifteen consecutive days (15 July to 29 July, 2019). The raw traffic flow data from the inductive loop detectors comprised the class-wise vehicular traffic flow for every 60 s for 24 h, from midnight to midnight. The description of these roadsites is in Table 2, and a sample of the traffic datasets collected from these roadsites is shown in Table 3. The four-way signalized road intersections connected to the N1 Allandale Interchange in which the traffic data was collected are:

- Brakfontein 1C N1 SB (Roadsite 1).
- Old Johannesburg Road SB off-ramp (Roadsite 2).
- Samrand Avenue SB off-ramp (Roadsite 3).
- Olifantsfont SB off-ramp (Roadsite 4).

Table 2. Description of the four-way signalized road intersection.

Road Intersections	Date	Distance (m)	Direction	Number of Lanes	Speed Limit (Km/h)	Number of Vehicles (Vehicles/h)
Roadsite 1	15 July 2019–27 July 2019	12.5	Southbound	7	120	1,097,152
Roadsite 2	15 July 2019–29 July 2019	9.40	Southbound	5	120	17,240,260
Roadsite 3	15 July 2019–29 July 2019	7.0	Southbound	7	120	12,448,023
Roadsite 4	15 July 2019–29 July 2019	3.70	Southbound	5	120	18,051,124

Table 3. Samples of the traffic datasets.

Light Vehicle			Long Truck			Medium Truck			Short Truck		
Speed (m/s)	Number of Light Vehicles	Time (s)	Speed (m/s)	Number of Long Trucks	Time (s)	Speed (m/s)	Number of Medium Trucks	Time (s)	Speed (m/s)	Number of Light Vehicles	Time (s)
115	1438	230	87	44	298	92	29	282	97	51	276
65	29,934	489	49	197	960	59	188	591	70	625	542
106	18,213	245	81	308	321	85	277	315	95	1056	278
103	223,44	255	82	321	316	85	263	308	97	865	271
109	3071	244	81	140	319	83	70	349	93	96	285
111	1234	237	82	115	313	84	35	306	95	54	277
60	28,844	565	52	258	833	52	206	750	65	635	586
107	24,793	241	83	338	310	88	332	298	99	1437	264
103	22,577	254	81	269	318	86	258	302	98	919	270
110	3432	241	81	162	320	84	91	315	95	94	278
113	1005	233	85	84	305	91	43	286	103	56	256
76	31,392	422	67	225	540	70	234	520	84	758	378
106	25,480	243	82	376	313	87	331	297	99	1503	266

3.8. Traffic Control Delay at Four-Way Signalized Road Intersections

To determine the control delay of vehicles at a road intersection, the queuing theory is used. Let us assume that we have an accumulation of vehicles at a road intersection waiting for the traffic lights to turn green. The accumulation of these vehicles at the road intersections with the time delay at the road intersection will form a triangle-like shape.

Let us use the mathematical expression of the area of the triangle. Figure 5, below, shows a sketch of four-way signalized road intersections.

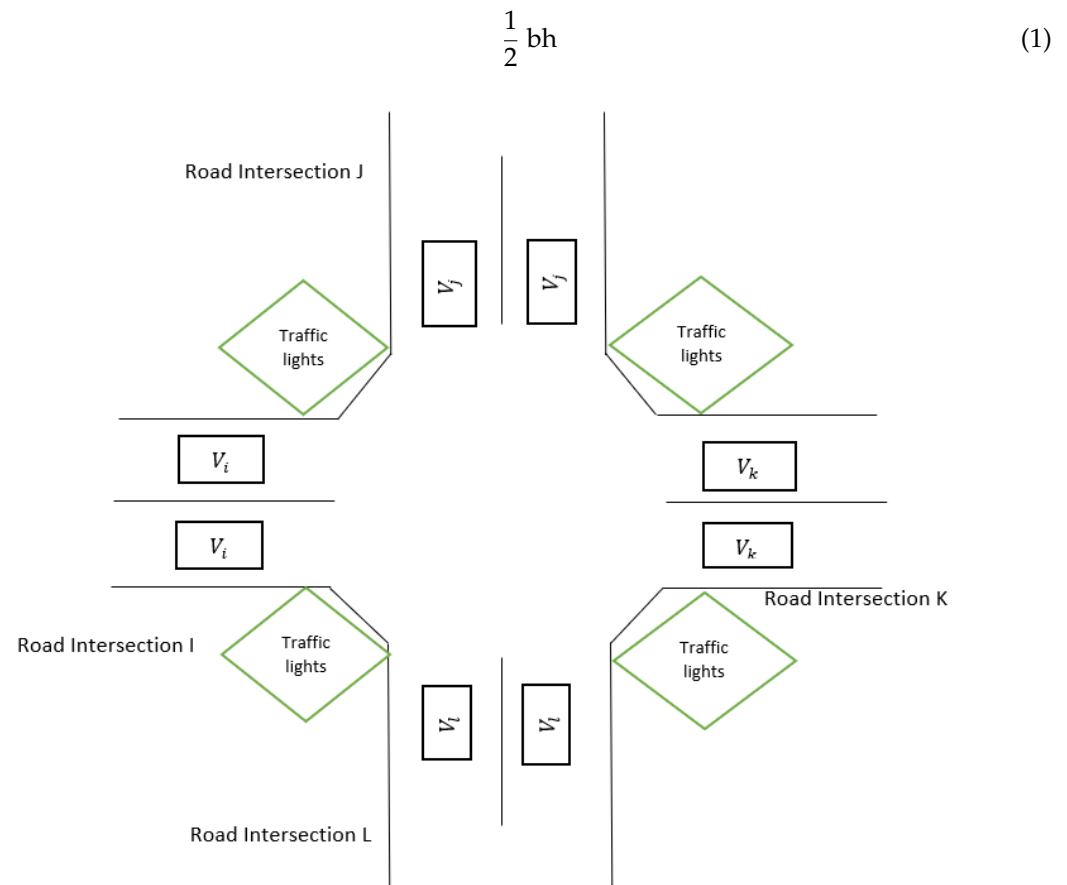


Figure 5. Four-way signalized road intersections.

Model Notation and Formulation

The following notations are used for the modelling of the traffic flow at signalized road intersections. The following assumptions were made based on the parameters used for the development of the model:

I = Intersection 1

J = Intersection 2

K = Intersection 3

L = Intersection 4

A_{ijkl} = 1 or 0 (the lane belongs to the intersection (i, j, k , and l) or otherwise).

B_{fijkl} = 1 or 0 (if road intersections i, j, k , and l have been controlled by phase f on the road intersection (i, j, k , and l)).

θ_{ijkl} = the traffic signal offset at road intersections i, j, k , and l .

T = the traffic flow analysis period duration (in hours).

EF_{ijkl} = the adjustment factor of the road intersections i, j, k , and l (hours).

C_{ijkl} = the traffic flow capacity of road intersections i, j, k , and l (vehicle/hour).

C = the traffic cycle length (seconds).

g_{ijkl} = the green time length at road intersections i, j, k , and l (seconds).

X_{ijkl} = road intersections i, j, k , and l 's degree of saturation (seconds).

d_{1ijkl} = intersections i, j, k , and l 's uniform delay (seconds/vehicle).

d_{2ijkl} = intersections i, j, k , and l 's increment delay (seconds/vehicle).

The control delay = $d(C)_{ijkl}$ is calculated as:

$$d(C)_{ijkl} = \sum_{ijkl \in K} A_{ijkl} (d_{1ijkl}(EF_{ijkl}) + d_{2ijkl}) \quad (2)$$

where,

$$d_{1ijkl} = \frac{0.5 \cdot C \cdot \left(1 - \frac{g_{ijkl}}{C}\right)^2}{1 - \min\left(1, X_{ijkl} \cdot \frac{g_{ijkl}}{C}\right)} \quad (3)$$

The average delay at each road intersection is $d(\theta)_{ijkl}$, which equals out to Equation (4).

$$d\theta_{ijkl} = \begin{cases} \sum_{k \in K} \frac{r_f}{g_f} (t_{ijkl} - \theta_{ijkl}) \cdot B_{f_{ijkl}} \cdot \text{if } (t_{ijkl} - g_{f_{ijkl}}) < \theta_{ijkl} < t_{ijkl} \\ (T_{ijkl} - \theta_{ijkl}) \text{ if } t_{ijkl} < \theta_{ijkl} < \sum_{k \in K} t_{ijkl} + (c - g_{f_{ijkl}}) B_{f_{ijkl}} \end{cases} \quad (4)$$

C_{ijkl} = the cycle lengths of intersections i, j, k , and l .

$g_{f_{ijkl}}$ = the green time lengths for intersections i, j, k , and l .

L_{ijkl} = the lost time of intersections i, j, k , and l .

θ_{ijkl} = the traffic flow conditions required for the calculation of the traffic signal offset of intersections i, j, k , and l .

The travel time t_{ijkl} of each vehicle on the road intersections (i, j, k , and l) is calculated as:

$$t_{ijkl} = t_{ijkl}(0) \left[1 + 0.15 \left(\frac{q_{ijkl}}{c_{ijl}} \right)^4 \right] \quad (5)$$

The free flow travel time $t_{ijkl}(0)$ of each vehicle on the intersections (i, j, k , and l) is calculated as:

$$t_{ijkl}(0) = \frac{I_{ijkl}}{V_{ijkl}} \quad (6)$$

Equation (6) validates the pre-existing equation related to the traffic flow at road intersections, i.e., that speed = $\frac{\text{distance}}{\text{time}}$.

Using time as the subject of the formula.

$$\text{Time} = \frac{\text{distance}}{\text{speed}} \quad (7)$$

In Equation (7), time is t_{ijkl} , distance is I_{ijkl} and speed is V_{ijkl} .

I_{ijkl} = the distance which has already been covered by the vehicles before arriving at the road intersections (i, j, k , and l) [m].

V_{ijkl} = the free-flow speed of the vehicles at each road intersection (i, j, k , and l) [m/s].

q_{ijkl} = the number of vehicles at each road intersection (i, j, k , and l) [veh/h].

C_{ijkl} = the road intersection's capacity (i, j, k , and l) [veh/h].

The primary aim of using this equation is to reduce the total travel time of vehicles at road intersections [TTT]. Let us assume that the number of vehicles reaching these road intersections during the simulation time is maximized.

$$\text{TTT} = \sum_{(i,j,k,l)} \text{TTT}_{i,j,k,l} = \sum_{(i,j,k,l) \in A} q_{ij,k,l} d_{ij,k,l} \quad (8)$$

The total delay (d_{ijkl}) of the vehicles at the road intersections is the sum of the control delay ($d(C)_{ijkl}$) at each intersection, the average delay, and the travel time of vehicles at each road intersection (t_{ijkl}).

$$d_{ijkl} = (d(C)_{ijkl}) + (d(\theta)_{ijkl}) + t_{ijkl} \quad (9)$$

The objective function of controlling real-time traffic flow at each road intersection in this study is minimized to the total travel time (TTT) at each road intersection.

To minimize TTT:

$$\sum (g_{fijkl}) = C_{ijkl} - L_{ijkl} \quad (10)$$

Through the combination of Equations (8) and (9), we get (10):

$$\text{TTT} = \sum_{(ijkl) \in A} q_{ijkl} (d(C)_{ijkl}) + (d(\theta)_{ijkl}) + t_{ijkl} \quad (11)$$

The relationship between the cycle lengths at each road intersection C_{ijkl} , the green time lengths at each road intersection (g_{fijkl}) and the lost time (L_{ijkl}) at each road intersection is explained by the constraints in (10) above. The condition required for the calculation of the signal offset (θ_{ijkl}) on the network is described by the constraint below (where

$$\sum (\theta)_{ijkl} + \sum (C_{ijkl} - (\theta)_{ijkl}) = n_h \cdot C_{ijkl} \quad (12)$$

and n_h is loop multiplication);

The constraint in Equation (13) defines the interval of the feasible cycle length values at each road intersection.

$$C_{min} \leq C_{ijkl} \leq C_{max} \quad (13)$$

$$g_{fmin} \leq g_{fijkl} \leq g_{fmax} \quad (14)$$

The constraint in Equations (13) and (14) above explains the interval of the feasible green time length values at each road intersection i, j, k , and l .

$$0 \leq (\theta)_{ijkl} \leq C_{ijkl} \quad (15)$$

The constraints in Equation (15) are the interval of the feasible traffic signal offset time length values at each road intersection.

3.9. Development of the ANN-PSO Model

Kennedy and Eberhart initially created the PSO method in the late 1990s [66]. This evolutionary algorithm benefits from a rapid rate of convergence when compared to other evolutionary algorithms, and it is a continuous process [67]. Therefore, it has been applied to perfection in many engineering applications [68–70]. In this technique, a cost function that is supposed to undergo minimization and maximization is defined. Then, a swarm of particles is created and distributed in the problem's 'D' dimensional space. Each particle comprise the problem variables, making it easier to calculate the cost fitness function. Conclusively, the velocity and position of each particle are updated with regard to Equation (17), until the PSO algorithm undergoes convergence.

$$\begin{aligned} V_i^{k+1} &= w \cdot V_i^k + C_1 \cdot r_1 \cdot (\rho_{best,i}^k - \rho_i^k) / \Delta t + C_2 r_2 \cdot (G_{best}^k - \rho_i^k) / \Delta t \\ \rho_i^{k+1} &= \rho_i^k + V_i^{k+1} \cdot \Delta t \end{aligned} \quad (16)$$

where,

i and k are known as the particle and number of iterations.

$\rho_i = \{\rho_{i1}, \rho_{i2}, \dots, \rho_{ij}, \dots, \rho_{iD}\}$ and $V_i = \{V_{i1}, V_{i2}, \dots, V_{ij}, \dots, V_{iD}\}$ are known as the position and velocity vectors.

$P_{best,i}^k = \{\rho_{i1}, \rho_{i2}, \dots, \rho_{ij}, \dots, \rho_{iD}\}$ and $G_{best}^k = \{g_1, g_2, \dots, g_D\}$ are the best position in terms of the i th particle, considering its history to iteration k .

$i = 1, 2, 3, \dots, N$ is the number of particles in the iteration, and D is the number of different problem dimensions.

Furthermore C_1 is a cognitive variable displaying the degree of the local search, but C_2 is a social variable for a global search. Besides this, r_1 and r_2 are two non-dependant variables uniformly distributed between zero and one, and 'w' is known as the inertia

weight applied in preserving the previous velocity of the particles during the process of optimization. Δt represents the time interval between the position and velocity when they are updated. Usually, the parameters during the updates are equal to 1. The artificial neural network model training is efficient when a problem has been minimized, which can be solved by applying a conventional or metaheuristic algorithm. However, in a hybrid artificial neural network trained by particle swarm optimization, the PSO functions to minimize errors during the ANN model training by knowing the optimum parameters for weights and biases of the ANN-PSO model [71]. Therefore, in this research, variables are known as the weights and biases, and the feasible space of the problems is dependent on the interval time at which these variables change. The cost function (fitness function) of the i th particle can be explained in terms of the root mean squared error [72]:

$$E(w_1, b_i) = \sqrt{\frac{1}{S} \sum_{k=1}^S \left[\sum_{l=1}^O \{T_{kl} - P_{kl}(w_1, b_i)\}^2 \right]} \quad (17)$$

where:

E = the cost fitness parameter

T_{kl} is the cost (fitness) value, and also the target value.

P_{kl} is the output predicted depending on the w_i (weights) and b_i (biases)

S is the number of training data.

O = the number of neurons.

To develop an ANN-PSO model, these steps must be adhered to:

1. Take into consideration the number of hidden neurons in the hidden layers and develop a neural network model using the initial weights and biases.
2. The reformation of the weights and biases, where there can be a representation of the location of a particle in a D-dimensional space of the problem, and D is the number of weights and biases.
3. During the iteration of each of the particles, the output values can be predicted and then mathematically calculated for the value of the cost function in Equation (18).
4. Update the location of particles in the PSO algorithm for a number of populations and iterations until the target output is fulfilled. In summary, there will be a minimization of the cost function.

The ANN-PSO used in this research study was developed in the MATLAB environment, with different artificial neural network architecture layers. The number of input variables is 13, which is also equal to the number of independent variables. The number of output neurons is also one, in tandem with the overall number of dependent variables. This study's number of neurons used varied between five (5) and ten (10), respectively. In this research study, we took into consideration the acceleration factors (C_1 and C_2), the swarm population size, and the number of neurons. The acceleration factors were selected randomly between 1 and 3, and the swarm population size was chosen from the options of 10, 20, 50, 100, 200, and 400. This research study considered 5, 6, 7, 8, 9, and 10 number neurons to achieve the best optimal results of the ANN-PSO model. The ANN-PSO model training will only be stopped or terminated when the objective function iteration has been fulfilled. The following benchmark was adhered to. The benchmark was:

1. A maximum iteration of 1000.
2. The training run will be terminated if the objective function is not up to a specific fixed parameter.

The number of neurons, the swarm population size, the accelerating factors C_1 and C_2 , and the time is taken to train each number of neurons was taken into consideration. The MATLAB codes used to develop the ANN-PSO model have been deposited in a GitHub repository. This is the link to the MATLAB codes: <https://github.com/Olayode1989/ANN-PSO-codes.git>, accessed on 1 September 2021. The ANN-PSO training and testing were carried out in the MATLAB environment by following the steps in Figure 6.

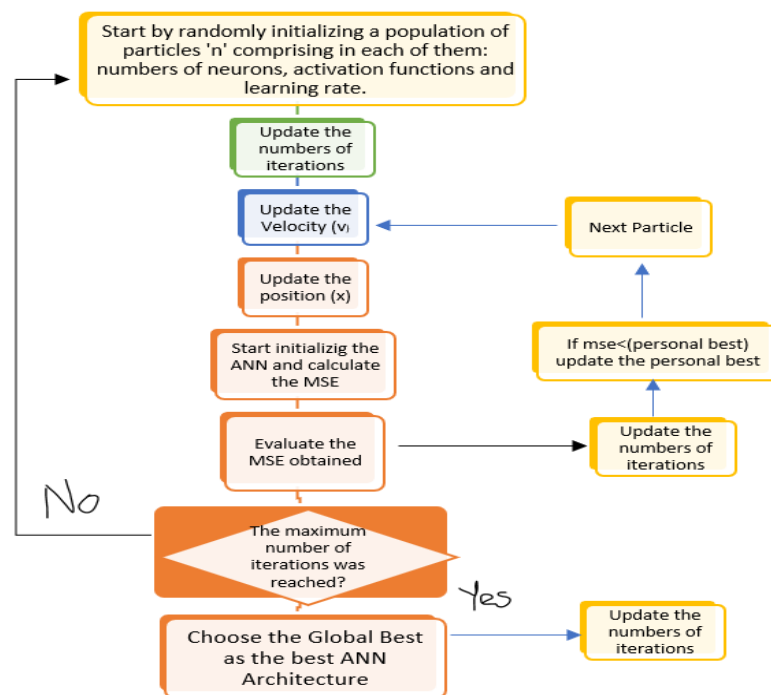


Figure 6. Development of the ANN-PSO Model.

3.10. Development of the ANN Model

ANN models are intelligent models motivated by the biological neural networks of both human beings and animals. This provides the learning patterns and high accuracy of model predictions of model problems in high-dimensional space [73–76]. An artificial neural network model can map the association between the inputs and outputs even if the datasets are complex or noisy. A Multilayer Perceptron (MLP) is not too complex. It possesses an effective feed-forward neural network model. An MLP neural network comprises an input layer, hidden layers (depending on the neural network model), and an output layer [77,78]. The input layer comprises of input parameters and transfers them to the neurons in the hidden layer. The value of these inputs, combined with a value of bias, is transformed by an activation function, as explained figuratively in Figure 7. Thereafter, the output signal is moved to the neurons in the next layer.

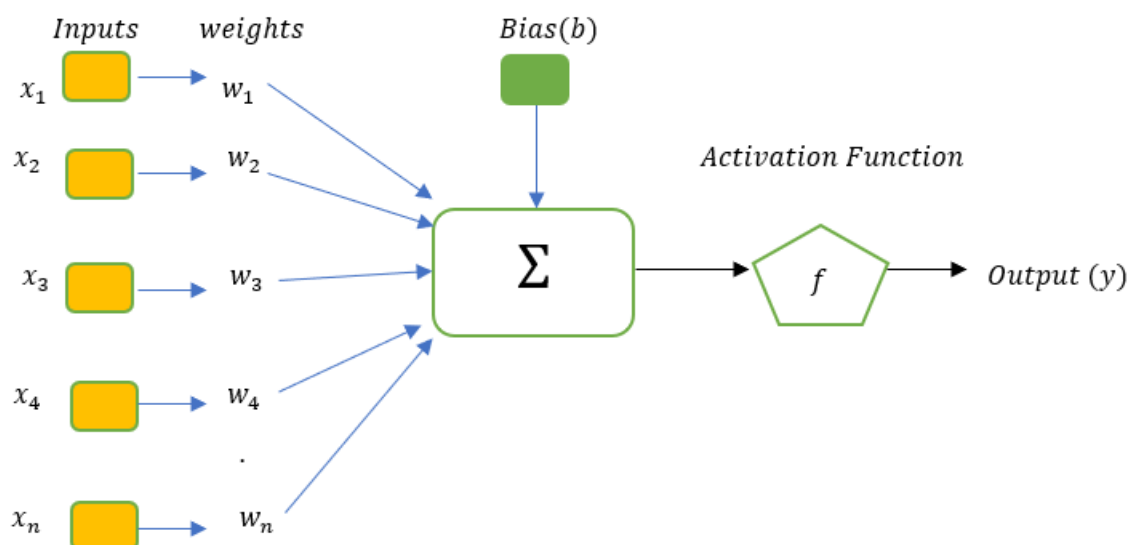


Figure 7. A neuron in an Artificial Neural Network.

The mathematical formulation of Figure 7 is shown below:

$$y_j = f\left(\sum_{i=1}^n w_{ij}x_i + b_j\right) \quad (18)$$

x_i and y_j are the nodal values in the preceding layer, I , and the present layer, j .

n is the overall number of the nodal values from the preceding layer.

w_{ij} and b_j are the weights and biases of the ANN.

The artificial neural network needs to be trained to display effective regression values performances. ANN model training means that the weights and biases of the ANN network are dependent on the minimal error between the relationships between the actual and network values. Therefore, the ANN network training process leads to the gradual minimization of the problem. Backpropagation (BP) algorithms are primarily applied for neural network training [79,80]. The Levenberg–Marquardt Algorithm (LMA) is usually identified as the fastest and most reliable training algorithm [81,82]; thus, we applied the backpropagation algorithm in this research study. When an artificial neural network is adequately trained in the MATLAB environment, it will function as a black-box model, explaining the relationship between a complex dataset, which comprises an input and output (irrespective of the number of variables). An ANN comprises complex mathematical processing units known as neurons. These neurons are situated in a place called the black box. These neurons will create a bond using weights and biases. Even though they consist of neurons, they also comprise of three significant layers, namely input layers, hidden layers, and output layers. The neurons are placed in the hidden and output layers, while the input layers do not contain neurons. In recent years, Artificial Neural Networks (ANN) have become a significant option in modelling due to their reduced computational time, efficient accuracy, and capability to show the relationships between inputs and outputs, depending on the data. The application of ANNs is limited to approximation; however, they also comprise classification, clustering, forecasting, pattern recognition, and image processing. There are different types of ANN depending on their architecture and model variables. The most widely used ANN is the backpropagation feedforward neural network, also known as a Multi-layer Perceptron (MLP), as shown in Figure 8.

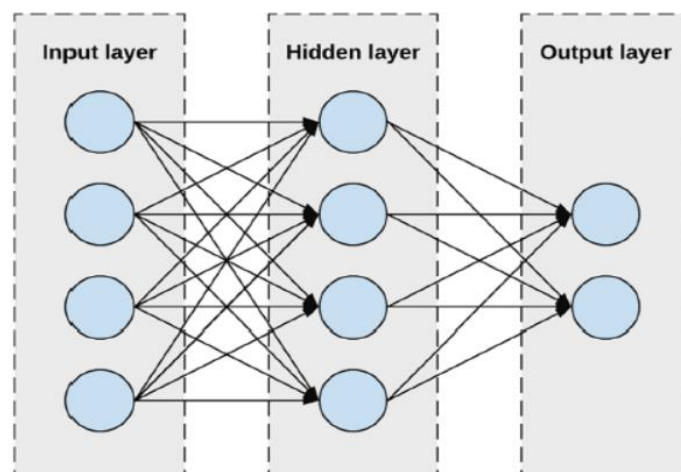


Figure 8. An example of a single hidden layer MLP architecture (4–4–2) consisting of four inputs, four neurons, and two outputs. Reprinted with permission from ref. [83]. Published by Elsevier B.V. Copyright © 2021 Elsevier Ltd. All rights reserved.

After the neural network toolbox is opened in MATLAB, the training will be conducted using the input traffic flow datasets and the output traffic datasets (traffic volume). The inputs are categorized into thirteen columns, while the output traffic datasets (traffic

volume) are in the same Microsoft excel sheet used for the input datasets (Table 1 shows the traffic data inputs and output). The traffic datasets' training was carried out to investigate the optimal traffic flow variables of various types of weights and biases of the ANN model. When the ANN model training has been carried out on the datasets, the neural network's performance is validated by applying independent variables. The ANN model training and testing are regarded as optimal when the fitness function characteristics, such as the R^2 , are of values that are closer to one.

4. Results and Discussions

4.1. Four-Way Signalized Road Intersection Vehicular Traffic Flow

The vehicular traffic flow of the four road intersections focused on in this research study is explained in the Appendix A section (Figure A1A–D). The traffic flow changes in these four roadsites were compared by plotting a bar chart pattern of the number of vehicles on each roadsite against the period of the day. The period of the day was divided into five periods within 24 h:

1 = 00:00:00 a.m.-04:59:59 a.m.

2 = 05:00:00 a.m.-09:59:59 a.m.

3 = 10:00:00 a.m.-14:59:59 p.m.

4 = 15:00:00 p.m.-19:59:59 p.m.

5 = 20:00:00 p.m.-23:59:59 p.m.

It is apparent from Figure A1A–D that there are very few vehicles on the road between 00:00:00 a.m. and 04:59:59 a.m. due to the number of vehicles on the road. Strong evidence of a high traffic volume was found during the day between 3 (10:00:00 a.m. to 14:59:59 p.m.) and 4 (15:00:00 p.m. to 19:59:59 p.m.) because a large volume of vehicles was found on each of the four intersections. The single most striking observation to emerge from the vehicular traffic flow bar chart interpretation below is that the number of vehicles on the road determines the traffic volume at any period of the day. Another observation is that there are no significant differences between the number of vehicles at period 5 (20:00:00 p.m. to 23:59:59 p.m.) for each road intersection.

4.2. Artificial Neural Network Model

In this research, an artificially intelligent model called an Artificial Neural Network (ANN) model was used to model the traffic flow at a four-way signalized road intersection, using the road transportation systems in South Africa as a case study. The traffic flow parameters measured include the number of vehicles on the road, traffic density, vehicular speed, traffic volume, and time, which were measured over a certain period of time. The location of the road intersections was densely populated and comprised of seven days of the week, which encompasses all the different likelihoods of what could hinder or interrupt the free-flowing movement of vehicles, thereby causing traffic congestion. Two hundred and fifty-nine (259) datasets were collected from these roadsites. These traffic datasets from each of the four road intersections were used for the ANN and ANN-PSO training, testing, and validation. The traffic dataset validation and testing were carried out to verify the efficiency of the ANN and ANN-PSO model. The ANN and ANN-PSO training, validation, and testing were executed in the MATLAB 2015a environment. The following traffic flow variables from the South Africa Road Transportation Network were used for the model training, validation, and testing:

1. **Network inputs:** The traffic density, number of light vehicles, average speed of light vehicles, time of day of light vehicles, the average speed of long trucks, time of day of long trucks, number of long trucks, the average speed of medium trucks, time of day

of medium trucks, number of medium trucks, number of short trucks, the average speed of short trucks and time of day of short trucks.

2. **Network Output:** Traffic volume.

The breakdown of how the traffic datasets were divided and used for the ANN training, validation, and testing is shown in Table 4.

Table 4. The breakdown of the roadsites' traffic datasets for the ANN model.

Roadsites.	Training	Validation	Testing	Total
Brakfontein 1C N1 SB (Roadsite 1)	36	15	10	61
Old Johannesburg Road SB off-ramp (Roadsite 2).	48	16	10	74
Samrand Avenue SB off-ramp (Roadsite 3).	41	13	10	64
Olifantsfnt SB off-ramp (Roadsite 4).	35	15	10	60
Total	160	59	40	259

Figure 9, below, shows the ANN model's neural network architecture used for the modelling of the traffic flow at the roadsites. There are 13 inputs and six hidden layers, and the one output shows the best artificial neural network model.

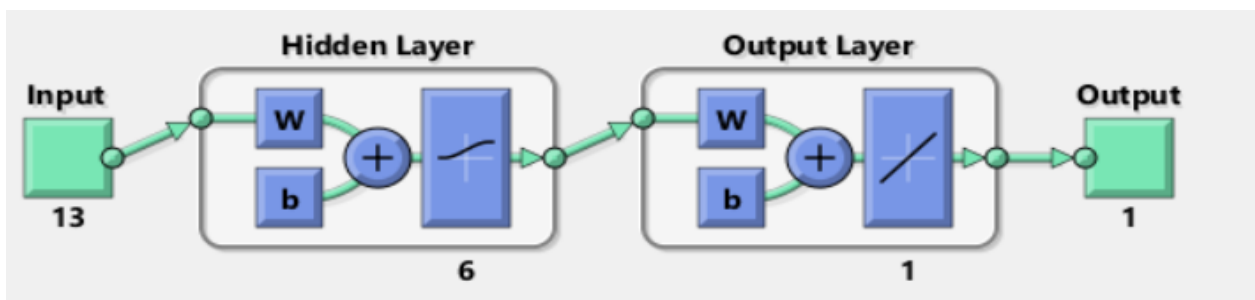


Figure 9. The neural network of the traffic datasets at the roadsites.

Figure 10 illustrates the best validation performance of the ANN model's training, testing, and validation at epoch 9.

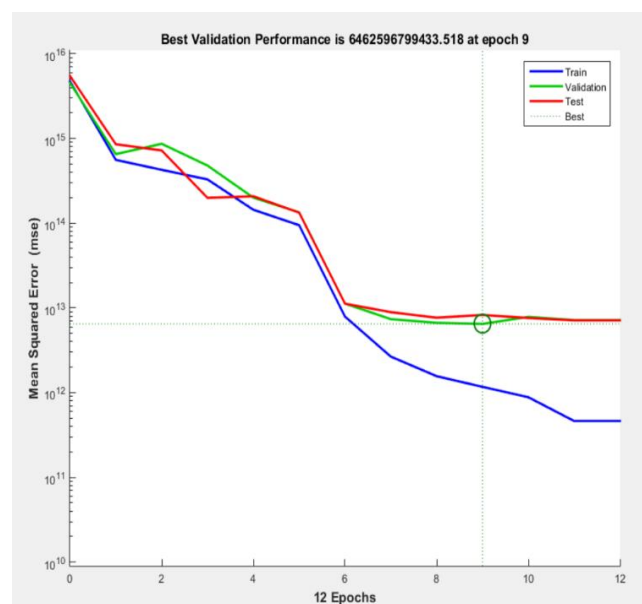


Figure 10. The validation performance for the ANN model of the traffic datasets at the roadsites.

The best validation performance network for the traffic datasets is shown in Figure 10. Figure 11 shows training, testing, and validation regression values of 0.96086, 0.99169, 0.97258, and an overall regression value of 0.96722 for the traffic datasets at the four road-sites. These results clearly show that the traffic data's inputs and outputs are well correlated.

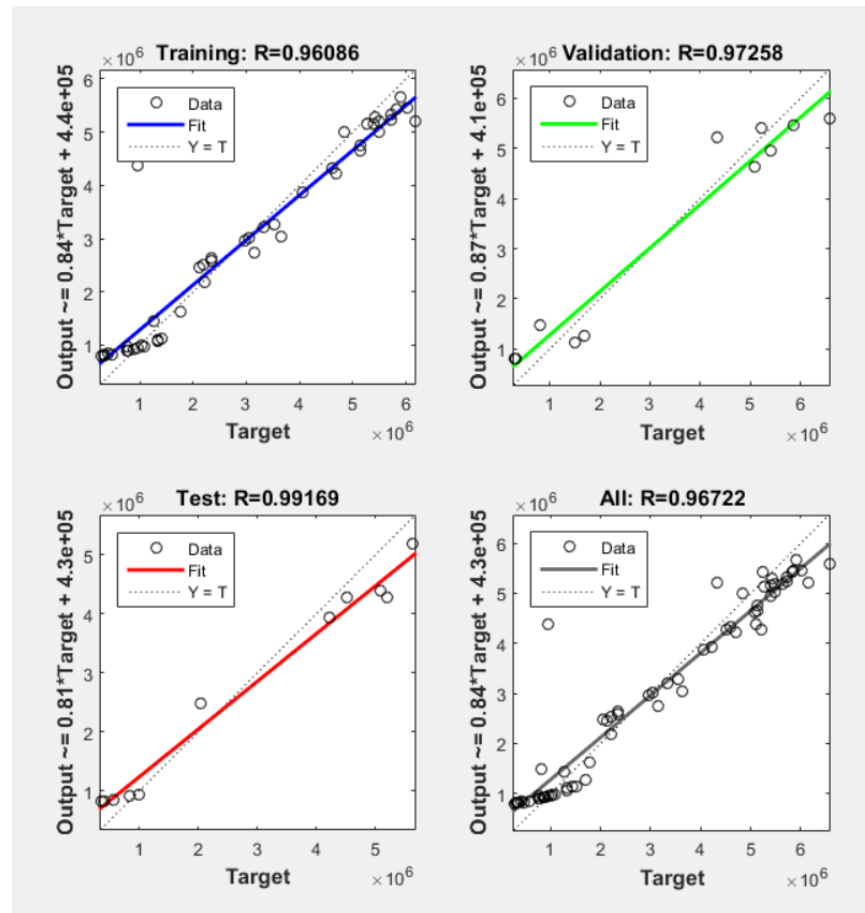


Figure 11. The ANN model results for the best prediction of the traffic datasets (13–6–1).

Figure 10 shows the training variations of the mean square error (MSE) of the training, testing, and validation data variations. The gradient epoch of the ANN performance of the roadside traffic datasets shows an epoch of 9 throughout the ANN model training and testing. The validation check of the ANN model was at 0.97258. This indicates the efficiency of the input and output variables. Figure 11, above, shows an overview of the corresponding traffic performance evaluation indices of the MSE and R^2 values for the ANN model training and testing of the traffic data. It is apparent from Figure 11 that the best optimum training performance was achieved when the number of hidden neurons was 6, i.e., 13–6–1. The single most striking observation to emerge from this ANN model is that the ANN parameters, number of hidden neurons, and number of epochs significantly affect the traffic flow dataset's performance prediction; the optimum networks obtained considering the traffic dataset's show a training performance of $R^2=0.96086$ and testing performance of $R^2=0.99169$, with six being the number of hidden neurons.

4.3. Artificial Neural Network—Particle Swarm Optimization Model

The breakdown of the way in which the traffic datasets were divided and used for the ANN-PSO training and testing is shown in Table 5 below.

Table 5. The breakdown of the roadside traffic datasets for the ANN-PSO training.

Roadsites	Training	Testing	Total
Brakfontein 1C N1 SB (Roadsite 1)	51	10	61
Old Johannesburg Road SB off-ramp (Roadsite 2).	64	10	74
Samrand Avenue SB off-ramp (Roadsite 3).	54	10	64
Olifantsfont SB off-ramp (Roadsite 4).	50	10	60
			259

The 259 traffic datasets from the four-way signalized road intersections were divided into 219 and 40 for training and testing. To achieve the best optimum output, a trial-and-error approach was used to discover the best value for the number of hidden nodes, iterations, and acceleration factors. Sigmoid and linear functions were used for the ANN-PSO model for the hidden and output node activation functions. The best optimal parameters for both the training and the testing of the performance of the ANN-PSO model of the traffic flow at the four intersections, as shown in Table 6, are:

Table 6. The parametric analysis of the hybrid ANN-PSO model training and testing results.

Number of Neurons	Swarm Population Size	C_1	C_2	Training (R^2)	MSE	Testing (R^2)
5	10	2.25	2	0.99600	22.228	0.9387
5	20	2.25	2	0.99392	27.429	0.9404
5	50	1.5	2.25	0.99966	19.522	0.7170
5	100	1	2.75	0.99863	15.463	0.9298
5	200	1.5	2	0.99951	23.388	0.9791
5	400	1.5	2	0.99952	23.161	0.9971
6	10	1	3	0.99127	34.088	0.8157
6	20	2	2.25	0.99629	21.404	0.8634
6	50	1	2.5	0.99948	24.253	0.9839
6	100	1	2.5	0.99917	32.025	0.9491
6	200	1	2.75	0.99769	17.855	0.8562
6	400	1	2.25	0.99961	20.907	0.9856
7	10	1.5	2.5	0.99324	29.150	0.4626
7	20	1	2.75	0.99807	16.893	0.9237
7	50	1	2.5	0.99939	26.448	0.2374
7	100	1	2.5	0.99906	34.934	0.9650
7	200	1.5	2.25	0.99893	38.076	0.9429
7	400	2	2	0.99847	15.881	0.8008
8	10	1	2.75	0.99697	19.679	0.7347
8	20	1	2.5	0.99944	25.211	0.9881
8	50	1.5	2.25	0.99955	22.507	0.9898
8	100	1	2.5	0.99974	17.675	0.9818
8	200	1	2.75	0.99943	25.388	0.9708
8	400	1	2.25	0.99974	17.496	0.9138
9	10	1	2.75	0.99307	29.775	0.3029
9	20	1	3	0.99206	32.091	0.9139
9	50	1.5	2.25	0.99895	37.571	0.7646
9	100	2	2	0.99911	33.780	0.9468
9	200	1.5	2.25	0.99807	16.890	0.8633
9	400	1	2.5	0.99973	17.962	0.9816
10	10	1	2.75	0.99900	36.389	0.7529
10	20	1.5	2.5	0.99871	15.261	0.8945
10	50	1.5	2.5	0.99896	37.306	0.6819
10	100	1	2.75	0.99741	18.641	0.8663
10	200	1	2.75	0.99920	31.178	0.9282
10	400	1.5	2.5	0.99799	17.088	0.9135

- (a) Number of hidden neurons = 5
- (b) Swarm population size = 400
- (c) Number of traffic datasets = 57
- (d) C_1 and $C_2 = 1.5$ and 2
- (e) Training (R^2) = 0.99952
- (f) Testing (R^2) = 0.99710

Figure 12a, below, shows the result of the ANN-PSO model training response of 0.99952, considering the number of hidden neurons, the number of input and output accelerating factors, and the swarm population sizes.

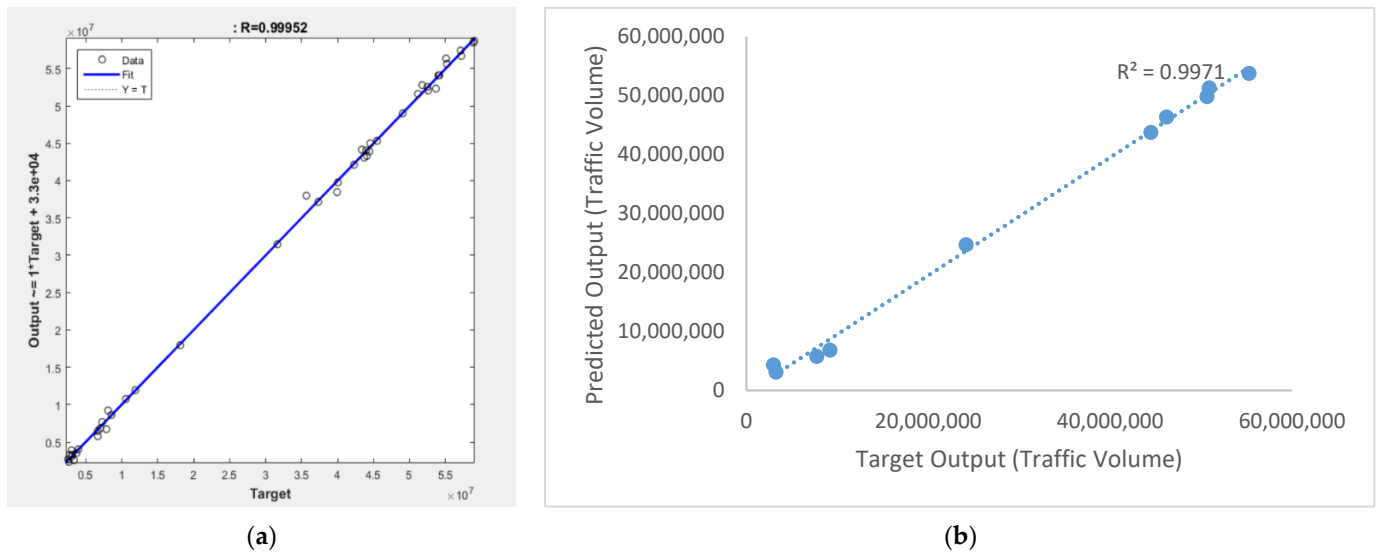


Figure 12. (a) ANN-PSO training response of the best performance network of the traffic datasets (13–5–1). (b) ANN-PSO testing response of the best performance network of the traffic datasets (13–5–1).

To evaluate the accuracy of the ANN-PSO model, the observed and predicted output of the traffic volume of the vehicles at each of the four roadsites were compared in Figure 12b, with the testing performance of the model being 0.9971. Table 6, above, shows that the corresponding traffic performance evaluation indices of the MSE and R^2 value for the training and testing traffic datasets have been presented. It can be discerned from the parametric study of the ANN-PSO hybrid model that the best optimum training performance was obtained when the total number of neurons was 5, the swarm population size was 400, and the best-achieving acceleration factors C_1 and C_2 were 1.5 and 2, respectively. An evaluative observation made from Table 6 is that the ANN-PSO's parameters affect the traffic congestion dataset's performance prediction. Besides this, the best training and testing results were not the same. Therefore, the optimum network obtained considering the traffic dataset's training performance is training $R = 0.99952$. The traffic dataset's best testing performance is $R^2 = 0.9971$, which has five hidden neurons. Figure 12a shows the training of the traffic data yield $R = 0.99952$, MSE = 23.161, while during the testing and validation of the results $R^2 = 0.9971$ (Figure 12b).

5. Conclusions and Future work

The current study aimed to determine the comparative traffic flow prediction performance between a heuristic ANN model and a hybrid ANN-PSO model in modelling vehicles' traffic flow at four-way signalized road intersections. A 259 traffic dataset database was collected from four signalized road intersections in South Africa's Road transportation system. Thirteen input parameters and one output parameter were taken into consideration. Based on these artificially intelligent approaches (ANN and ANN-PSO) used for the traffic flow data, the following conclusions can be drawn from the present study:

1. One of the most significant findings to emerge from this study is that the comparison of the ANN-PSO model and ANN model has shown that the ANN-PSO model is far more accurate, easy to use, and efficient than the ANN model, with a testing performance of 0.9971, compared to the ANN model's testing performance of 0.99169.
2. This study also suggests that a Neural Network comprising five (5) neurons is the best-performing neural network during the ANN-PSO model training of the traffic datasets.
3. The investigation of the use of the ANN model to model self-driving vehicles at four-way signalized road intersections has shown that the best training performance of the traffic datasets was achieved when the number of hidden neurons is 6, which leads to training (R) 0.96086, testing (R) 0.99169, validation (R) 0.97258, and All (R) 0.96722.
4. The most apparent findings from this research study are that the efficiency of the traffic dataset's prediction performance depends on the total number of input variables. Further observation also showed that the number of parameters of the input variables determined the predictor model's accuracy (ANN and ANN-PSO model).
5. The evidence from this study suggests that ANN and ANN-PSO are reliable predictors of the traffic flow of vehicles at a signalized road intersection.
6. An implication of the results of this research study is the possibility that transportation researchers and civil engineers could apply the ANN and ANN-PSO model used in this research study in the development of ways to improve road transportation mobility through technologically advanced traffic management techniques.
7. This research study extends our knowledge of traffic flow modelling and the application of soft computing techniques in vehicular traffic flow at a signalized road intersection.

It is recommended that further research be undertaken in the following areas:

1. A natural progression of this work is to determine whether transportation researchers can use expanded and robust real-time traffic data to achieve a more profound impact of these traffic variables on traffic flow prediction and thus improve the traffic flow prediction efficiency and reliability.
2. A possible area of research is the application of statistical analysis in the validation of the ANN and ANN-PSO model results of this study.
3. Another possible area of future research would be to investigate the possibility that, due to traffic data's sequential nature irrespective of whether it is traffic data from developing or developed countries, it would be possible to conduct research by following the deep learning methods explained by [37], such as artificial bee colony optimization, grasshopper optimization algorithm, and bat algorithm. These methods can all be tested and compared with the results obtained from this paper to determine which one has a better testing performance (R^2).
4. Further research regarding the prediction performance of ANN and ANN-PSO (using convergent plots) in the modelling of the vehicular traffic flow at an un-signalized road intersection would be interesting.

Author Contributions: Supervision, L.K.T. and M.O.O.; writing—original draft, I.O.O.; writing—review and editing, L.K.T., M.O.O. and A.S. All authors have read and agreed to the published version of the manuscript.

Funding: This research received no external funding.

Institutional Review Board Statement: Not Applicable.

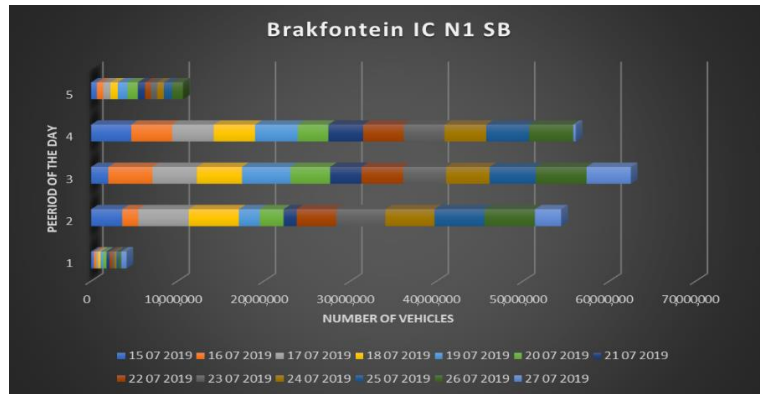
Informed Consent Statement: Not Applicable.

Data Availability Statement: The traffic datasets used for this research study are available upon reasonable request from the South Africa Ministry of Transportation and South African National Roads Agency Limited (SANRAL). The MATLAB codes used to develop the ANN-PSO model have been deposited in a GitHub repository. This is the link to the MATLAB codes: <https://github.com/Olayode1989/ANN-PSO-codes.git> (accessed on 1 September 2021).

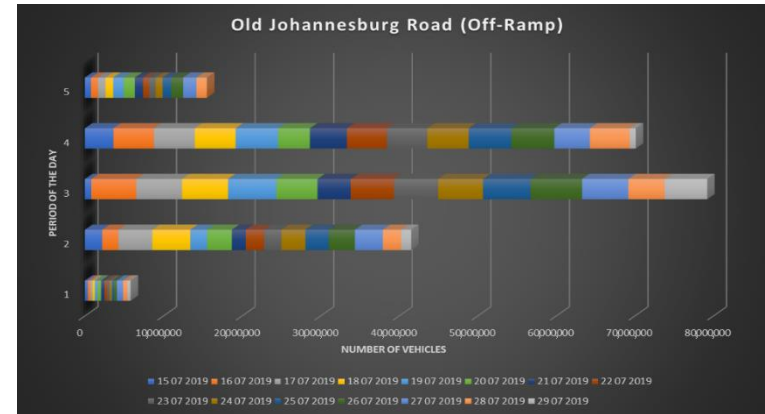
Acknowledgments: We would like to appreciate the South Africa Ministry of Transportation for the use of their traffic data.

Conflicts of Interest: The authors declare no conflict of interest. The funders had no role in the study's design; in the collection, analyses, or interpretation of data; in the writing of the manuscript, or in the decision to publish the results.

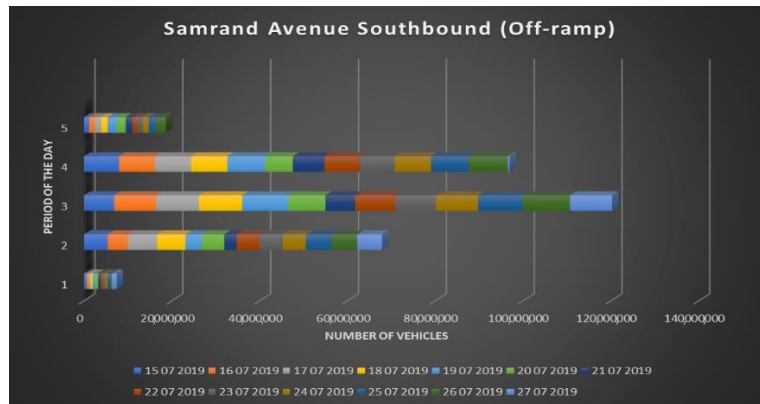
Appendix A



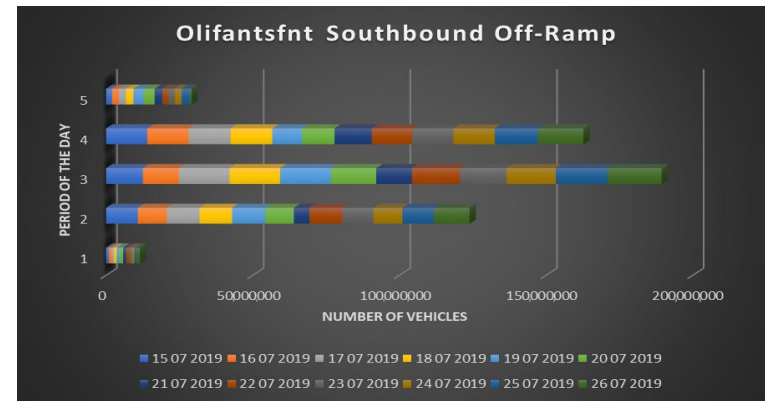
(A) Roadsite 1



(B) Roadsite 2



(C) Roadsite 3



(D) Roadsite 4

Figure A1. The vehicular traffic flow of the four road intersections.

References

1. Jabbarpour, M.R.; Zarrabi, H.; Khokhar, R.H.; Shamshirband, S.; Choo, K.-K.R. Applications of computational intelligence in vehicle traffic congestion problem: A survey. *Soft Comput.* **2018**, *22*, 2299–2320. [\[CrossRef\]](#)
2. Hamed, M.M.; Al-Masaeid, H.R.; Said, Z.M.B. Short-term prediction of traffic volume in urban arterials. *J. Transp. Eng.* **1995**, *121*, 249–254. [\[CrossRef\]](#)
3. Karlaftis, M.G.; Vlahogianni, E.I. Statistical methods versus neural networks in transportation research: Differences, similarities and some insights. *Transp. Res. Part C Emerg. Technol.* **2011**, *19*, 387–399. [\[CrossRef\]](#)
4. Smola, A.J.; Schölkopf, B. A tutorial on support vector regression. *Stat. Comput.* **2004**, *14*, 199–222. [\[CrossRef\]](#)
5. Zivot, E.; Wang, J. Vector autoregressive models for multivariate time series. *Modeling Financ. Time Ser. S-Plus* **2006**, 385–429. [\[CrossRef\]](#)
6. Huang, M.-L. Intersection traffic flow forecasting based on ν -GSVR with a new hybrid evolutionary algorithm. *Neurocomputing* **2015**, *147*, 343–349. [\[CrossRef\]](#)
7. Westgate, B.S.; Woodard, D.B.; Matteson, D.S.; Henderson, S.G. Travel time estimation for ambulances using Bayesian data augmentation. *Ann. Appl. Stat.* **2013**, *7*, 1139–1161. [\[CrossRef\]](#)
8. Davis, G.A.; Nihan, N.L. Nonparametric regression and short-term freeway traffic forecasting. *J. Transp. Eng.* **1991**, *117*, 178–188. [\[CrossRef\]](#)
9. Defferrard, M.; Bresson, X.; Vandergheynst, P. Convolutional neural networks on graphs with fast localized spectral filtering. *Adv. Neural Inf. Process. Syst.* **2016**, *29*, 3844–3852.
10. Lazzús, J.A.J.M.; Modelling, C. Neural network-particle swarm modeling to predict thermal properties. *Math. Comput. Model.* **2013**, *57*, 2408–2418. [\[CrossRef\]](#)
11. Yusiong, J.P.T. Optimizing artificial neural networks using cat swarm optimization algorithm. *Int. J. Intell. Syst. Appl.* **2012**, *5*, 69. [\[CrossRef\]](#)
12. Celtek, S.A.; Durdu, A.; Ali, M.E.M. Real-time traffic signal control with swarm optimization methods. *Measurement* **2020**, *166*, 108206. [\[CrossRef\]](#)
13. D’Andrea, E.; Marcelloni, F. Detection of traffic congestion and incidents from GPS trace analysis. *Expert Syst. Appl.* **2017**, *73*, 43–56. [\[CrossRef\]](#)
14. Gidófalvi, G. Scalable selective traffic congestion notification. In Proceedings of the Fourth ACM SIGSPATIAL International Workshop on Mobile Geographic Information Systems, Bellevue, WA, USA, 3 November 2015; pp. 40–49.
15. Anwar, T.; Vu, H.L.; Liu, C.; Hoogendoorn, S.P. Temporal tracking of congested partitions in dynamic urban road networks. *Transp. Res. Rec.* **2016**, *2595*, 88–97. [\[CrossRef\]](#)
16. Liang, Z.; Wakahara, Y. Real-time urban traffic amount prediction models for dynamic route guidance systems. *EURASIP J. Wirel. Commun. Netw.* **2014**, *2014*, 1–13. [\[CrossRef\]](#)
17. Kong, X.; Xu, Z.; Shen, G.; Wang, J.; Yang, Q.; Zhang, B. Urban traffic congestion estimation and prediction based on floating car trajectory data. *Future Gener. Comput. Syst.* **2016**, *61*, 97–107. [\[CrossRef\]](#)
18. Ma, X.; Yu, H.; Wang, Y.; Wang, Y. Large-scale transportation network congestion evolution prediction using deep learning theory. *PLoS ONE* **2015**, *10*, e0119044. [\[CrossRef\]](#)
19. Davoodi, N.; Soheili, A.R.; Hashemi, S.M. A macro-model for traffic flow with consideration of driver’s reaction time and distance. *Nonlinear Dyn.* **2016**, *83*, 1621–1628. [\[CrossRef\]](#)
20. Qian, Z.S.; Li, J.; Li, X.; Zhang, M.; Wang, H. Modeling heterogeneous traffic flow: A pragmatic approach. *Transp. Res. Part B Methodol.* **2017**, *99*, 183–204. [\[CrossRef\]](#)
21. Van Der Voort, M.; Dougherty, M.; Watson, S. Combining Kohonen maps with ARIMA time series models to forecast traffic flow. *Transp. Res. Part C Emerg. Technol.* **1996**, *4*, 307–318. [\[CrossRef\]](#)
22. Williams, B.M.; Hoel, L.A. Modeling and forecasting vehicular traffic flow as a seasonal ARIMA process: Theoretical basis and empirical results. *J. Transp. Eng.* **2003**, *129*, 664–672. [\[CrossRef\]](#)
23. Zhao, L.; Song, Y.; Zhang, C.; Liu, Y.; Wang, P.; Lin, T.; Deng, M.; Li, H. T-gcn: A temporal graph convolutional network for traffic prediction. *IEEE Trans. Intell. Transp. Syst.* **2019**, *21*, 3848–3858. [\[CrossRef\]](#)
24. Sun, Y.; Leng, B.; Guan, W. A novel wavelet-SVM short-time passenger flow prediction in Beijing subway system. *Neurocomputing* **2015**, *166*, 109–121. [\[CrossRef\]](#)
25. Zhang, J.; Cui, J.; Zhong, H.; Chen, Z.; Liu, L. PA-CRT: Chinese remainder theorem based conditional privacy-preserving authentication scheme in vehicular ad-hoc networks. *IEEE Trans. Dependable Secur. Comput.* **2019**, 722–735. [\[CrossRef\]](#)
26. Hong, W.-C. Traffic flow forecasting by seasonal SVR with chaotic simulated annealing algorithm. *Neurocomputing* **2011**, *74*, 2096–2107. [\[CrossRef\]](#)
27. Chang, H.; Lee, Y.; Yoon, B.; Baek, S. Dynamic near-term traffic flow prediction: System-oriented approach based on past experiences. *IET Intell. Transp. Syst.* **2012**, *6*, 292–305. [\[CrossRef\]](#)
28. Xia, D.; Wang, B.; Li, H.; Li, Y.; Zhang, Z. A distributed spatial-temporal weighted model on MapReduce for short-term traffic flow forecasting. *Neurocomputing* **2016**, *179*, 246–263. [\[CrossRef\]](#)

29. Moretti, F.; Pizzuti, S.; Panzieri, S.; Annunziato, M. Urban traffic flow forecasting through statistical and neural network bagging ensemble hybrid modeling. *Neurocomputing* **2015**, *167*, 3–7. [[CrossRef](#)]
30. Xu, X.; Zhang, X.; Liu, X.; Jiang, J.; Qi, L.; Bhuiyan, M.Z.A. Adaptive computation offloading with edge for 5G-envisioned internet of connected vehicles. *IEEE Trans. Intell. Transp. Syst.* **2020**, 5213–5222. [[CrossRef](#)]
31. Xu, X.; Liu, X.; Xu, Z.; Dai, F.; Zhang, X.; Qi, L. Trust-oriented IoT service placement for smart cities in edge computing. *IEEE Internet Things J.* **2019**, *7*, 4084–4091. [[CrossRef](#)]
32. Zhang, Y.; Yin, C.; Lu, Z.; Yan, D.; Qiu, M.; Tang, Q. Recurrent Tensor Factorization for time-aware service recommendation. *Appl. Soft Comput.* **2019**, *85*, 105762. [[CrossRef](#)]
33. Lv, Y.; Duan, Y.; Kang, W.; Li, Z.; Wang, F.-Y. Traffic flow prediction with big data: A deep learning approach. *IEEE Trans. Intell. Transp. Syst.* **2014**, *16*, 865–873. [[CrossRef](#)]
34. Koesdwiady, A.; Soua, R.; Karray, F. Improving traffic flow prediction with weather information in connected cars: A deep learning approach. *IEEE Trans. Veh. Technol.* **2016**, *65*, 9508–9517. [[CrossRef](#)]
35. Ma, X.; Tao, Z.; Wang, Y.; Yu, H.; Wang, Y. Long short-term memory neural network for traffic speed prediction using remote microwave sensor data. *Transp. Res. Part C: Emerg. Technol.* **2015**, *54*, 187–197. [[CrossRef](#)]
36. Menezes Jr, J.M.P.; Barreto, G.A. Long-term time series prediction with the NARX network: An empirical evaluation. *Neurocomputing* **2008**, *71*, 3335–3343. [[CrossRef](#)]
37. Yang, B.; Sun, S.; Li, J.; Lin, X.; Tian, Y. Traffic flow prediction using LSTM with feature enhancement. *Neurocomputing* **2019**, *332*, 320–327. [[CrossRef](#)]
38. Tian, Y.; Zhang, K.; Li, J.; Lin, X.; Yang, B. LSTM-based traffic flow prediction with missing data. *Neurocomputing* **2018**, *318*, 297–305. [[CrossRef](#)]
39. Zhao, Z.; Chen, W.; Wu, X.; Chen, P.C.; Liu, J. LSTM network: A deep learning approach for short-term traffic forecast. *IET Intell. Transp. Syst.* **2017**, *11*, 68–75. [[CrossRef](#)]
40. LeCun, Y.; Bengio, Y.; Hinton, G. Deep learning. *Nature* **2015**, *521*, 436–444. [[CrossRef](#)]
41. Zhang, Y.; Wang, K.; He, Q.; Chen, F.; Deng, S.; Zheng, Z.; Yang, Y. Covering-based web service quality prediction via neighborhood-aware matrix factorization. *IEEE Trans. Serv. Comput.* **2019**. [[CrossRef](#)]
42. Zhang, Y.; Yin, C.; Wu, Q.; He, Q.; Zhu, H. Location-aware deep collaborative filtering for service recommendation. *IEEE Trans. Syst. Man Cybern. Syst.* **2019**, *51*, 3796–3807. [[CrossRef](#)]
43. Zhang, J.; Zheng, Y.; Qi, D. Deep spatio-temporal residual networks for citywide crowd flows prediction. In Proceedings of the AAAI Conference on Artificial Intelligence, San Francisco, CA, USA, 4–9 February 2017.
44. Vlahogianni, E.I.; Karlaftis, M.G.; Golias, J.C. Short-term traffic forecasting: Where we are and where we’re going. *Transp. Res. Part C Emerg. Technol.* **2014**, *43*, 3–19. [[CrossRef](#)]
45. Li, Y.; Shahabi, C. A brief overview of machine learning methods for short-term traffic forecasting and future directions. *Sigspatial Spec.* **2018**, *10*, 3–9. [[CrossRef](#)]
46. Nagy, A.M.; Simon, V. Survey on traffic prediction in smart cities. *Pervasive Mob. Comput.* **2018**, *50*, 148–163. [[CrossRef](#)]
47. Singh, A.; Shadan, A.; Singh, R. Traffic forecasting. *Int. J. Sci. Res.* **2019**, *7*, 1565–1568.
48. Boukerche, A.; Wang, J. Machine Learning-based traffic prediction models for Intelligent Transportation Systems. *Comput. Netw.* **2020**, *181*, 107530. [[CrossRef](#)]
49. Majumder, S.; Kar, S.; Pal, T. Rough-fuzzy quadratic minimum spanning tree problem. *Expert Syst.* **2019**, *36*, e12364. [[CrossRef](#)]
50. Majumder, S.; Kar, S.; Pal, T. Uncertain multi-objective Chinese postman problem. *Soft Comput.* **2019**, *23*, 11557–11572. [[CrossRef](#)]
51. Lana, I.; Del Ser, J.; Velez, M.; Vlahogianni, E. Road traffic forecasting: Recent advances and new challenges. *IEEE Intell. Transp. Syst. Mag.* **2018**, *10*, 93–109. [[CrossRef](#)]
52. Tedjopurnomo, D.A.; Bao, Z.; Zheng, B.; Choudhury, F.; Qin, A. A survey on modern deep neural network for traffic prediction: Trends, methods and challenges. *IEEE Trans. Knowl. Data Eng.* **2020**. [[CrossRef](#)]
53. Ye, J.; Zhao, J.; Ye, K.; Xu, C. How to build a graph-based deep learning architecture in traffic domain: A survey. *IEEE Trans. Intell. Transp. Syst.* **2020**, 1–21. [[CrossRef](#)]
54. Xie, P.; Li, T.; Liu, J.; Du, S.; Yang, X.; Zhang, J. Urban flow prediction from spatiotemporal data using machine learning: A survey. *Inf. Fusion* **2020**, *59*, 1–12. [[CrossRef](#)]
55. Kirby, H.R.; Watson, S.M.; Dougherty, M.S. Should we use neural networks or statistical models for short-term motorway traffic forecasting? *Int. J. Forecast.* **1997**, *13*, 43–50. [[CrossRef](#)]
56. Smith, B.L.; Demetsky, M.J. Traffic flow forecasting: Comparison of modeling approaches. *J. Transp. Eng.* **1997**, *123*, 261–266. [[CrossRef](#)]
57. Vlahogianni, E.I.; Golias, J.C.; Karlaftis, M.G. Short-term traffic forecasting: Overview of objectives and methods. *Transp. Rev.* **2004**, *24*, 533–557. [[CrossRef](#)]
58. Vlahogianni, E.I.; Karlaftis, M.G.; Golias, J.C. Statistical methods for detecting nonlinearity and non-stationarity in univariate short-term time-series of traffic volume. *Transp. Res. Part C Emerg. Technol.* **2006**, *14*, 351–367. [[CrossRef](#)]
59. Zheng, W.; Lee, D.-H.; Shi, Q. Short-term freeway traffic flow prediction: Bayesian combined neural network approach. *J. Transp. Eng.* **2006**, *132*, 114–121. [[CrossRef](#)]
60. Sun, S.; Zhang, C. The selective random subspace predictor for traffic flow forecasting. *IEEE Trans. Intell. Transp. Syst.* **2007**, *8*, 367–373. [[CrossRef](#)]

61. Stathopoulos, A.; Dimitriou, L.; Tsekeris, T. Fuzzy modeling approach for combined forecasting of urban traffic flow. *Comput.-sAided Civ. Infrastruct. Eng.* **2008**, *23*, 521–535. [[CrossRef](#)]
62. Tan, M.-C.; Wong, S.C.; Xu, J.-M.; Guan, Z.-R.; Zhang, P. An aggregation approach to short-term traffic flow prediction. *IEEE Trans. Intell. Transp. Syst.* **2009**, *10*, 60–69.
63. Kyte, M.; Urbanik, T. *Traffic Signal Systems Operations and Design: An Activity-Based Learning Approach. Isolated Intersections*; Pacific Crest Software Inc.: Tualatin, OR, USA, 2012; ISBN 13.
64. Kumar, K.; Parida, M.; Katiyar, V. Short term traffic flow prediction for a non urban highway using artificial neural network. *Procedia-Soc. Behav. Sci.* **2013**, *104*, 755–764. [[CrossRef](#)]
65. Goves, C.; North, R.; Johnston, R.; Fletcher, G. Short term traffic prediction on the UK motorway network using neural networks. *Transp. Res. Procedia* **2016**, *13*, 184–195. [[CrossRef](#)]
66. Kennedy, J.; Eberhart, R.C. A discrete binary version of the particle swarm algorithm. In Proceedings of the 1997 IEEE International Conference on Systems, Man, and Cybernetics. Computational Cybernetics and Simulation, Orlando, FL, USA, 12–15 October 1997; pp. 4104–4108. [[CrossRef](#)]
67. Khan, K.; Sahai, A. A comparison of BA, GA, PSO, BP and LM for training feed forward neural networks in e-learning context. *Int. J. Intell. Syst. Appl.* **2012**, *4*, 23. [[CrossRef](#)]
68. Bao, Y.; Xiong, T.; Hu, Z. PSO-MISMO modeling strategy for multistep-ahead time series prediction. *IEEE Trans. Cybern.* **2013**, *44*, 655–668. [[PubMed](#)]
69. Hasanipannah, M.; Noorian-Bidgoli, M.; Armaghani, D.J.; Khamesi, H. Feasibility of PSO-ANN model for predicting surface settlement caused by tunneling. *Eng. Comput.* **2016**, *32*, 705–715. [[CrossRef](#)]
70. Mohandes, M.A. Modeling global solar radiation using Particle Swarm Optimization (PSO). *Sol. Energy* **2012**, *86*, 3137–3145. [[CrossRef](#)]
71. Nguyen, H.; Moayedi, H.; Foong, L.K.; Al Najjar, H.A.H.; Jusoh, W.A.W.; Rashid, A.S.A.; Jamali, J. Optimizing ANN models with PSO for predicting short building seismic response. *Eng. Comput. Int. J. Simul.-Based Eng.* [[CrossRef](#)]
72. Chau, K.W. Application of a PSO-based neural network in analysis of outcomes of construction claims. *Autom. Constr.* **2007**, *16*, 642–646. [[CrossRef](#)]
73. Jain, A.K.; Mao, J.; Mohiuddin, K.M. Artificial neural networks: A tutorial. *Comput. Commun.* **1996**, *29*, 31–44. [[CrossRef](#)]
74. Priddy, K.L.; Keller, P.E. *Artificial Neural Networks: An Introduction*; SPIE Press: Bellingham, WA, USA, 2005; Volume 68.
75. Nguyen, H.; Bui, X.-N.; Bui, H.-B.; Mai, N.-L. A comparative study of artificial neural networks in predicting blast-induced air-blast overpressure at Deo Nai open-pit coal mine, Vietnam. *Neural Comput. Appl.* **2020**, *32*, 3939–3955. [[CrossRef](#)]
76. Nguyen, H.; Drebenstedt, C.; Bui, X.-N.; Bui, D.T. Prediction of blast-induced ground vibration in an open-pit mine by a novel hybrid model based on clustering and artificial neural network. *Nat. Resour. Res.* **2020**, *29*, 691–709. [[CrossRef](#)]
77. Alizamir, M.; Sobhanardakani, S. An Artificial Neural Network-Particle Swarm Optimization (ANN-PSO) approach to predict heavy metals contamination in groundwater resources. *Jundishapur J. Health Sci.* **2018**, *10*. [[CrossRef](#)]
78. Nguyen, H.; Bui, X.-N.; Tran, Q.-H.; Le, T.-Q.; Do, N.-H. Evaluating and predicting blast-induced ground vibration in open-cast mine using ANN: A case study in Vietnam. *SN Appl. Sci.* **2019**, *1*, 1–11. [[CrossRef](#)]
79. Olayode, I.; Tartibu, L.; Okwu, M.; Uchechi, U. Intelligent transportation systems, un-signalized road intersections and traffic congestion in Johannesburg: A systematic review. *Procedia CIRP* **2020**, *91*, 844–850. [[CrossRef](#)]
80. Olayode, I.O.; Tartibu, L.K.; Okwu, M.O. Traffic flow Prediction at Signalized Road Intersections: A case of Markov Chain and Artificial Neural Network Model. In Proceedings of the 2021 IEEE 12th International Conference on Mechanical and Intelligent Manufacturing Technologies (ICMIMT); pp. 287–292. [[CrossRef](#)]
81. Olayode, O.; Tartibu, L.; Okwu, M. Application of Artificial Intelligence in Traffic Control System of Non-autonomous Vehicles at Signalized Road Intersection. *Procedia CIRP* **2020**, *91*, 194–200. [[CrossRef](#)]
82. Olayode, I.O.; Tartibu, L.K.; Okwu, M.O. Application of Fuzzy Mamdani Model for Effective Prediction of Traffic Flow of Vehicles at Signalized Road Intersections. In Proceedings of the 2021 IEEE 12th International Conference on Mechanical and Intelligent Manufacturing Technologies (ICMIMT), Cape Town, South Africa, 13–15 May 2021; pp. 219–224. [[CrossRef](#)]
83. Jawad, J.; Hawari, A.H.; Zaidi, S.J. Artificial Neural Network Modeling of Wastewater Treatment and Desalination Using Membrane Processes: A Review. *Chem. Eng. J.* **2021**, 129540. [[CrossRef](#)]